



## Article

# Design and Study of a Spindle-Shaped Fry Head-to-Tail Orientation Device

Jianping Li <sup>1,2,3,\*</sup>, Chen Li <sup>1,3</sup> , Congcong Li <sup>1,3</sup>, Wei Luo <sup>1,2</sup>, Kang Wu <sup>1,3</sup> , Songming Zhu <sup>1,2,3</sup> and Zhangying Ye <sup>1,2,3,\*</sup>

<sup>1</sup> College of Biosystems Engineering and Food Science, Zhejiang University, Hangzhou 310058, China

<sup>2</sup> Key Laboratory of Equipment and Informatization in Environment Controlled Agriculture, Ministry of Agriculture and Rural Affairs, Hangzhou 310058, China

<sup>3</sup> Key Laboratory of Intelligent Equipment and Robotics for Agriculture of Zhejiang Province, Hangzhou 310058, China

\* Correspondence: jpli@zju.edu.cn (J.L.); yzyzju@zju.edu.cn (Z.Y.)

**Abstract:** The head-to-tail orientation of spindle-shaped fry is an important part of automated vaccine injection. The fry's automatic orientation helps reduce labor and improve efficiency during the automated injection. This paper designed an electromagnetic vibration fry orientation device for grass carp fry, measured its friction characteristics with three different materials in scales and against scales, analyzed the kinematic characteristics of the fry on the electromagnetic vibration feeder, and clarified the main factors affecting fry transport. It used the trough's inclination angle, amplitude, and material as the test factors, whereas the orientation success rate and orientation rate were used as the evaluation index. Orthogonal combination tests were carried out with 90–150 mm grass carp fry as the research object to obtain reasonable parameter combinations. The results showed that the best orientation effect was achieved when the surface of the trough was a silicone film with many bumps, the inclination of the plate spring was  $\beta = 15^\circ$ , the inclination of the trough plane was  $\theta_y = -4^\circ$ , and the amplitude  $A = 0.7$  mm. In this parameter combination, the directional device was tested and verified. The targeted success rate was  $\varepsilon = 95.5\%$ , and the direction rate was  $\eta = 0.87$  tail/s. The device could meet the requirements of the head and tails during the mechanized injection of the fry.

**Keywords:** spindle-shaped fry; head-to-tail orientation; orthogonal test; parameter optimization



**Citation:** Li, J.; Li, C.; Li, C.; Luo, W.; Wu, K.; Zhu, S.; Ye, Z. Design and Study of a Spindle-Shaped Fry Head-to-Tail Orientation Device. *Fishes* **2023**, *8*, 143. <https://doi.org/10.3390/fishes8030143>

Academic Editor: Yang Liu

Received: 16 January 2023

Revised: 11 February 2023

Accepted: 16 February 2023

Published: 28 February 2023



**Copyright:** © 2023 by the authors. Licensee MDPI, Basel, Switzerland. This article is an open access article distributed under the terms and conditions of the Creative Commons Attribution (CC BY) license (<https://creativecommons.org/licenses/by/4.0/>).

## 1. Introduction

Vaccination has become one of the most important disease prevention and control strategies. It has become a normative requirement for modern aquaculture [1–3]. Fish body orientation, including head-to-tail and abdomen-to-back orientation, is an important part of automated vaccine injection. It simplifies the design and layout of automatic fish vaccination systems and reduces mortality [4].

Head-to-tail orientation is the alignment of the head and tail of the fish along the length of the body [5]. The main methods include mechanical methods, electronic methods and other methods. The mechanical method mainly uses properties such as the position of the center of gravity, friction and shape. Xiang et al. reported on the head-to-tail orientation of commercial fish based on the position of the center of gravity of freshwater fish close to the head, using a tilted vibrating table [6–8]. Webster and Bergman [9] achieved head and tail orientation using the center of gravity of a fish close to the head under the action of the cyclonic flow in an inverted conical vessel. Furthermore, Zhang [10] used the different positions of the fish's center of gravity on the baseboard to allow forward and reverse fish to enter different conveyor belts according to the difference in the frictional force between the scales and the inverse scales of freshwater fish.

On the other hand, Wan et al. and Lin achieved head-to-tail orientation through the reciprocating motion of conveyor belts and bamboo strips [11,12]. Moreover, Xu took

advantage of the different shapes of the head and tail of the fish body and set up a pressing wheel and a sorting plate to achieve head and tail orientation [13]. Electronic method: Pegoraro and Wang used sensors to detect fish head orientation and combined them with corresponding actuators to achieve fish head-to-tail orientation [14,15]. Other methods, such as those by Andresen et al. [16] and Wenzel [17], were based on the liquid bridge principle [18], utilizing the different mass distribution of the fish body along the body length direction and using a moist cylindrical stick to achieve the head-to-tail orientation of scaleless fish. Therefore, based on the previous literature, research on head-to-tail orientation has mainly focused on marine and commercial fish, and there have been few studies on the head-to-tail orientation of fry. In addition, the equipment for commercial fish has a large vibration amplitude and takes a long time to orientate, so it is not suitable for the orientation of the head and tail of the fry.

Furthermore, vibration orientation is also commonly used in agricultural seeding processes, and agricultural sowing processes, such as the orientation of garlic cloves [19,20], rice sowing [21,22] and corn seed sowing [23,24]. In this paper, according to the principle of vibration orientation, the orientation mechanism is analyzed using the friction and vibration characteristics of the fish body, and the key parameters are determined. Thus, this study aims to solve the problem of the head-to-tail orientation of fry and to provide technical support for automated fish vaccination.

## 2. Materials and Methods

### 2.1. Design of the Orientation Device and Its Working Principle

#### 2.1.1. Structural Design of Orientation Device

The structure of the head-to-tail orientation device is shown in Figure 1. The experimental platform for this study used an electromagnetically driven vibratory feeder. It controlled the voltage frequency and waveform of the electromagnet coil so that the electromagnet generated periodic electromagnetic force and the armature was attracted. As a result, the leaf spring was periodically deformed and drove the high-frequency vibration of the trough. The trough was installed on the vibrator through the X-axis angle adjustment plate and the Y-axis angle adjustment plate. The trough plane could be rotated to a certain angle along the X-axis and Y-axis, respectively, and the size was 380 mm × 260 mm.

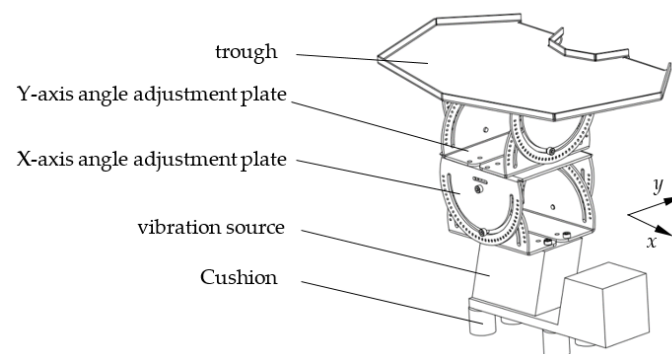


**Figure 1.** Head-to-tail orientation device.

#### 2.1.2. Working Principle

The force of the fry on the inclined surface of the trough is shown in Figure 2. The figure shows that the body length direction and the sliding direction are vertical. The center of mass of the fish body is point O. In the figure (Figure 2),  $f_1$  and  $f_2$  are the combined forces of the frictional forces on the fishhead portion on the left side of the center of mass and the fishtail portion on the right side of the center of mass, respectively.  $G_1$  is the component force of the fish's gravity at the center of mass in the direction of sliding. When the fry is on the trough's slope,  $G_1 > f_1 + f_2$ , the fish will slide down the table. When the torque of  $f_2$  on the fry center of mass is greater than the torque of  $f_1$  on the fry center of mass, the fish will

turn as they slide down the slope of the trough. The design achieves the head-to-front and tail-to-back state and completes the head-to-tail orientation.

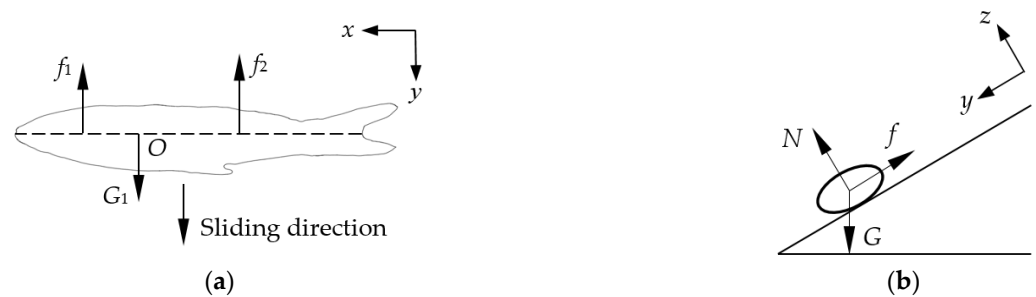


**Figure 2.** Diagram of the forces on the fish. (a) Force in x-y plane. (b) Force in y-z plane.

In addition, the friction angle of the fish body with the scale direction is smaller than the friction angle of the anti-scale direction. Therefore, it is conducive to the stable sliding of the fish body on the slope of the trough after the head and tail are oriented. To slide more stably, the difference between the friction angle with the scale and the friction angle against the scale needs to be larger. In this research, silicone with bumps, a 316L stainless steel plate and a PU conveyor belt were selected. It adopted the same measurement method as Wan et al. [6] to measure its friction angle, and the measurement results are shown in Table 1.

**Table 1.** Friction angle measurement of fry.

Materials	Scale	Reverse Scale	Difference
316L	12.9°	22.5°	9.6°
PU	38.3°	42.5°	4.2°
Silicone	25.2°	45.1°	19.9°

When the fry slid on the three different contact surfaces along the scale direction and the anti-scale direction, respectively, the measured friction angles were different. They all showed that the friction angle in the anti-scale direction was greater than the friction angle in the scale direction. The difference between the friction angle with the scale and the friction angle against the scale was the largest measured on the silicone surface with many bumps, followed by the 316L plate, and the difference between the friction angle on the PU conveyor belt was the smallest.

Furthermore, the fishtail can be seen as a stretchable membrane with mucus. When the contact surface is smooth, there is a layer of liquid bridge between the fishtail and the contact surface [25]. Furthermore, when the fry slide along the anti-scale direction, the fishtail gradually expands, and the area of the liquid bridge increases, making the fishtail and contact surfaces more adhesive. This is another reason for its frictional anisotropy.

## 2.2. Analysis of the Head and Tail Orientation Process of Fry

During the movement of the fry, it was affected by the dynamic parameters of the electromagnetic vibrating feeder. It would also be affected by the friction coefficient between the fry and the trough and the geometric parameters of the electromagnetic vibration feeder, such as the installation angle of the trough, the installation angle of the leaf spring, etc. When the electromagnetic vibrating feeder adopted different parameters, the basic motion state of the material on the trough could be divided into the following four states: static state, forward slip, reverse slip and throwing movement [26].

### 2.2.1. Fry Movement Status

To explore the factors affecting the movement of fry on the electromagnetic vibrator, a kinematic analysis was carried out. At any point on the trough plane, the displacement

along the direction perpendicular to the leaf spring could be approximated as a simple harmonic motion.

$$S = A \sin \omega t \quad (1)$$

where  $A$  denotes the amplitude of the vibration,  $\omega$  denotes the vibration's angular frequency and  $t$  represents the time.

After the first and second derivations of the time  $t$  in Equation (1), the velocity  $v$  and acceleration  $a$  are obtained:

$$v = \omega A \cos \omega t \quad (2)$$

$$a = -\omega^2 A \sin \omega t \quad (3)$$

Assuming that the fry and the trough were initially stationary, the trough was in the positive half of the movement when the forward slip started. In that, when  $\sin \omega t > 0$ , the fry was always in contact with the plane of the trough, and the fry slid positively toward the left side with respect to the trough. The force analysis sketch was shown in Figure 3.

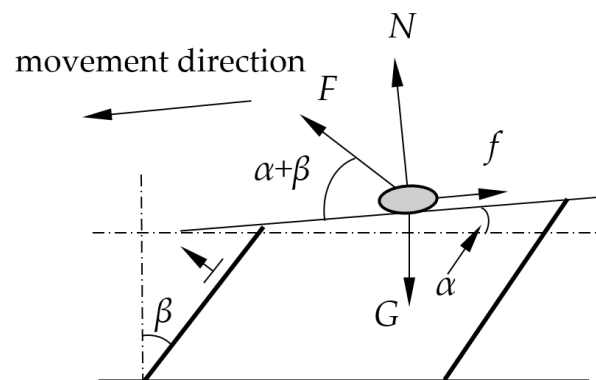


**Figure 3.** Sketch of forward slip force analysis.

The system of equilibrium equations was as follows:

$$\begin{cases} F \cos(\alpha + \beta) + G \sin \alpha - f = ma \\ F \sin(\alpha + \beta) + N - G \cos \alpha = 0 \end{cases} \quad (4)$$

Here:  $\alpha$  is the angle between the trough and the horizontal plane.  $\beta$  is the angle between the plate spring and the vertical direction.  $(\alpha + \beta)$  is the vibration direction angle.  $f$  is the frictional force.  $N$  is the support force.  $F$  is the inertia force in the direction of the vertical plate spring, and  $a$  is the acceleration of the fry relative to the trough. For the convenience of analysis, let  $f = \mu N$ ,  $\mu = \tan \varphi$ .  $\varphi$  is the kinetic friction angle.

From Equations (2)–(4), we can obtain:

$$ma = \frac{[F \cos(\varphi - (\alpha + \beta)) + G \sin(\alpha - \beta)]}{\cos \varphi} \quad (5)$$

To ensure that the fry do not slide by themselves, generally  $|\alpha| < \varphi$ , and  $F > 0$ ,  $\cos \varphi > 0$ . If the fry starts to slide forward from the static state,  $a > 0$ , there are formulas:

$$\cos(\varphi - (\alpha + \beta)) > 0 \quad (6)$$

$$F > \frac{G \sin(\varphi - \alpha)}{\cos(\varphi - (\alpha + \beta))} \quad (7)$$

The vibration intensity of the electromagnetic vibrating feeder is  $K$ , which is obtained from Equation (7).

$$K > \frac{\sin(\alpha - \varphi)}{\cos(\varphi - (\alpha + \beta))} = K_{\text{forward slide}} \quad (8)$$

From Equation (8), it can be seen that the vibration intensity  $K$  of the electromagnetic feeder is greater than the forward slip critical vibration intensity  $K_{fs}$  ( $K_{fs}$  represents  $K_{\text{forward slide}}$ ). The fry begins to slip forward relative to the trough plane.

At the beginning of the reverse slip, the trough is in the negative half of the motion,  $\sin \omega t < 0$ . The force analysis is shown in Figure 4. The balanced equation is as follows:

$$\begin{cases} F \cos(\alpha + \beta) + G \sin \alpha + f = ma \\ F \sin(\alpha + \beta) + N - G \cos \alpha = 0 \end{cases} \quad (9)$$

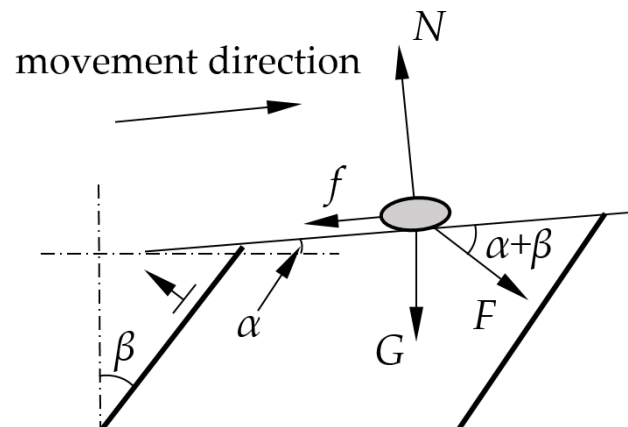


**Figure 4.** Sketch of reverse slip force analysis.

Solve it in the same way:

$$K > \frac{\sin(\alpha + \varphi)}{\cos(\varphi + \alpha + \beta)} = K_{\text{reverse slide}} \quad (10)$$

From Equation (10), it can be seen that the vibration intensity  $K$  of the electromagnetic feeder is greater than the reverse slip critical vibration intensity  $K_{rs}$  ( $K_{rs}$  represents  $K_{\text{reverse slide}}$ ). Then, the fry begins to slip reverse relative to the trough plane.

In the state of throwing motion, the fry leaves the plane of the trough, that is, when  $N < 0$ . The fry may be thrown up during the positive and negative half of the vibration. Further, when the trough is in the positive half cycle of motion (i.e.,  $\sin \omega t > 0$ ), combined with the formula from Equation (4), we receive:

$$K > \frac{\cos \alpha}{\sin(\alpha + \beta)} = K_{\text{throwing vibration}} \quad (11)$$

When the trough is in the negative half of the motion, and  $\sin \omega t < 0$ , another relation can be obtained from the formula of Equation (9):

$$K > -\frac{\cos \alpha}{\sin(\alpha + \beta)} = K_{\text{throwing vibration}} \quad (12)$$

When the vibration intensity  $K$  of the electromagnetic feeder is greater than the throwing critical vibration intensity  $K_{tv}$  ( $K_{tv}$  represents  $K_{\text{throwing vibration}}$ ), the fry will be thrown up relative to the trough plane.

In one vibration cycle, according to the relationship between the vibration intensity  $K$  of the electromagnetic vibratory feeder and the critical characteristic values  $K_{fs}$ ,  $K_{rs}$  and  $K_{tv}$  for each state of motion, the fry can achieve different movement states in the feeder.

## 2.2.2. Fry Assemblage Movement Status

The above analysis showed that the relationship between different vibration intensities  $K$  and the critical vibration intensities of different motion states corresponded to the motion

states of different fry. The critical vibration intensity was also affected by factors such as the friction coefficient  $\varphi$  between the fry and the trough plane, the angle  $\alpha$  between the trough plane and the horizontal plane, and the leaf spring installation angle  $\beta$ . In addition, the friction between the fry and the trough differs in the along-scale and anti-scale directions. Therefore, fry with different orientations present various combined motion states under different parameters within one vibration period.

To avoid confusion, it was stipulated that the initial position of the fry in the plane of the trough with the head to the left and the tail to the right was forward. That was the same direction as the positive sliding. The initial position of the fry was the head to the right, and the tail to the left was backward. That was the same direction as the reverse sliding. In a vibration period, the combined motion state of the fry sliding relative to the trough plane was obtained from the combination of four basic motion states. The friction angle  $\varphi_{ws}$  of the fry with the scale direction was smaller than the friction angle  $\varphi_{as}$  of the anti-scale direction, meaning that the fry slide more easily in the direction of the scales and with more difficulty in the direction of the opposite scales. With this feature, when the parameters of the electromagnetic vibration feeder were selected within a suitable range, fry with their heads and tails facing different directions would slide up the trough in the direction of their respective scales. Thus, it achieved the head-to-tail orientation of the fry.

In practice, the mounting angle  $\beta$  of the plate spring was generally fixed at a certain angle. For small electromagnetic vibrating feeders, generally  $\beta = 10\sim 20^\circ$ ; here, we selected  $\beta = 15^\circ$ . Therefore, assuming that the trough plane was a silicone surface with many bumps, by combining Equations (8) and (10)–(12), a diagram of the relationship between the vibration intensity  $K$ , the installation angle of the trough  $\alpha$ , the friction angle  $\varphi_{ws}$  with the scale, the friction angle  $\varphi_{as}$  against the scale and the movement state of the fry can be obtained.

It can be seen from Figure 5 that the critical vibration intensity of fry with the scale was smaller than the critical vibration intensity in the direction against the scale, whether it was forward slipping or reverse slipping.  $K_{fs-\varphi_{ws}} < K_{fs-\varphi_{as}}$ ,  $K_{rs-\varphi_{ws}} < K_{rs-\varphi_{as}}$ . Therefore, when the vibration intensity  $K$  gradually increased, the fry would first slide toward the direction of the scale. As the vibration intensity  $K$  further increased, there would be sliding against the scale direction.

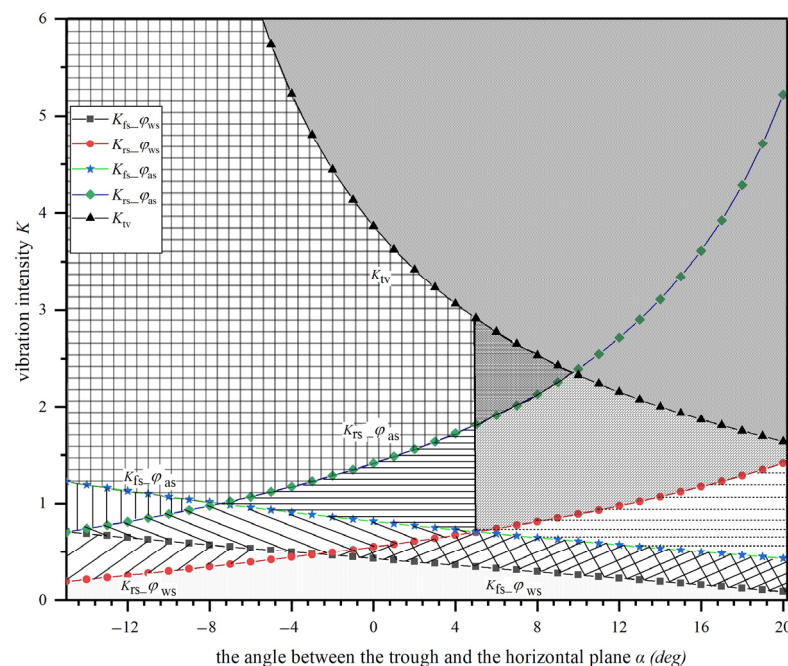


Figure 5. Fry Movement Relationship Chart.



In the same sliding direction, the fry would slide more easily along the scale direction than against the scale direction. Then, fish placed forward are more easily distinguished than those placed backwards. When the difference  $\Delta$  between the fry with the scale friction angle  $\varphi_{ws}$  and against the scale friction angle  $\varphi_{as}$  is larger, the trend is more obvious. This is reflected in the diagram as the larger the forward and backward sliding area.

### 2.3. Simulation Calculation of Fry Speed Velocity

The fry were tender and vulnerable, and slipping was the preferred mode of movement. The motion state analysis was only within a single vibration cycle. The results were accurate only if the forward and reverse slip motions did not affect each other. If there were both forward and reverse slip motions, the forward and reverse slip motions would interact with each other as the period of vibration increased. This would result in a non-zero velocity when the acceleration was zero, affecting its final combined state of motion.

First, a certain moment  $t_z$  and  $v_0$  when the fry slipped in the positive half of the vibration was recorded. Then, the forward slip velocity  $v$  of the fry relative to the trough at time  $t$  was:

$$v = \int_{t_z}^t a dt + v_0 \quad (13)$$

Substituting Equation (13) into Equation (5) gives:

$$v = \left[ \cos \omega t_z - \cos \omega t + \frac{g \sin(\alpha - \varphi)}{\omega^2 A \cos((\alpha + \beta) - \varphi)} (\omega t - \omega t_z) \right] \frac{\omega A \cos((\alpha + \beta) - \varphi)}{\cos \varphi} + v_0 \quad (14)$$

The fry could slide forward when the critical positive sliding start angle had a solution. Calculate the fry's average velocity  $v$  positive slip relative to the trough when the initial positive slip velocity  $v_0 = 0$  and the initial phase angle  $\theta_z$ . The forward slip angle at the end of the forward slip was  $\theta_{z'}$ , the time was  $t_{z'}$  and  $v = 0$ . We can obtain from Equation (14):

$$\cos \theta_z - \cos \theta_{z'} + \sin_{FS}(\theta_z - \theta_{z'}) = 0 \quad (15)$$

$\theta_{z'}$  can be obtained by solving the transcendental Equation (15) by geometric or numerical solution. Therefore, the average velocity  $v_1$  of the fry relative to the forward slip of the trough was:

$$v_{FS} = \left[ \frac{\cos^2 \theta_z - \cos^2 \theta_{z'}}{2 \sin \theta_{FS}} - (\sin \theta_{z'} - \sin \theta_z) \right] \frac{\omega A \cos((\alpha + \beta) - \varphi)}{2\pi \cos \varphi} \quad (16)$$

The average velocity  $v_2$  of the fry sliding backwards relative to the trough was:

$$v = \left[ \frac{\cos^2 \theta_z - \cos^2 \theta_{z'}}{2 \sin \theta_{FS}} - (\sin \theta_{z'} - \sin \theta_z) \right] \frac{\omega A \cos((\alpha + \beta) + \varphi)}{2\pi \cos \varphi} \quad (17)$$

It was observed that Equations (16) and (17) only had the difference of the sign in front of  $\varphi$ . Its positive and negative signs correspond to the direction of the frictional force. Then, the following equation unified the average velocity  $v_{slip}$  of the fry sliding relative to the trough.

$$v_S = v_S(0, \theta_0, \theta, MK \cdot \varphi, \omega, A, \alpha, \beta) \quad (18)$$

In the formula,  $v_0$  is the initial velocity of the slip,  $\theta_0$  is the initial phase angle,  $\theta$  is the phase angle at the end and  $MK$  is the sign position. When  $MK = -1$ , the fry slips forward and the friction is negative; when  $MK = 1$ , the fry slips backward and the friction is positive.

It can be seen from Figure 5 that the fry may have a forward slip and reverse slip at the same time. The average speed at which the fry finally appeared to visually slip:

$$v_S = v_{fs} + v_{rs} \quad (19)$$

Whether the fry shows a positive or reverse slip, in the end, depends on the positive or negative value of  $v_1$ . Head-to-tail orientation is considered successful when  $v_f > 0$  and  $v_r < 0$ , and the fry in the forward direction slides out with the head facing left.

$$V = \begin{cases} \frac{2v_f|v_r|}{v_f+|v_r|} & , v_f > 0 \text{ and } v_r < 0 \\ 0, & \text{Other conditions} \end{cases} \quad (20)$$

In addition, considering that efficiency needed to be taken into account in the process of head-to-tail orientation, the slip efficiency index  $\eta$  was defined.

$$\eta = \frac{v}{K} \quad (21)$$

In the formula,  $v$  is the fry's sliding speed relative to the trough's plane when the vibration intensity is  $K$ .

When the excitation frequency  $\omega$  was fixed, the vibration intensity  $K$  was proportional to amplitude  $A$ . The amplitude  $A$  and vibration intensity  $K$  were the upper and lower axes, respectively, and the mean directional velocity  $V$  was the left axis. Simulations based on Equations (20) and (21) were carried out to obtain the relationship between the average orientation velocity  $V$  for different contact surfaces, trough plane mounting angles  $\alpha$ , vibration intensity  $K$ , amplitude  $A$  and fry head-to-tail orientation.

When the contact surface was a silicone plane with many bumps on the surface, the simulation of the slip velocity was calculated by taking the interval of  $-12^\circ \leq \alpha \leq 4^\circ$  in combination with the analysis above, as shown in Figure 6.

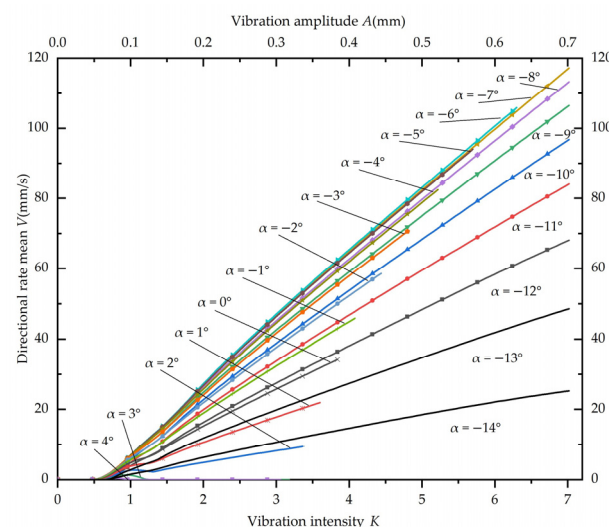


**Figure 6.** The trough is silicone with many small protrusions.

When the installation angle of the trough plane  $\alpha \geq -7^\circ$ , the maximum vibration intensity  $K_{\max}$  of the fry sliding motion decreased with the increase in  $\alpha$ . The vibration intensity range for the fry to perform a sliding movement was gradually compressed, and the maximum value of the average directional velocity of the fry decreased. When  $\alpha \geq 3^\circ$ , the backwards-placed fry slid together with the forward-placed fry in the forward direction, and their average directional velocity was zero.

When the trough plane installation angle  $\alpha < -7^\circ$ , with the increase in  $\alpha$ , the maximum value of the average orientation speed of fry increased, and the slip efficiency index  $\eta$  increased. When  $\alpha < -15^\circ$ , the forward-placed fry slides together with the backwards-placed fry toward the reverse direction with zero average directional velocity.

When  $\alpha = -6^\circ$ , the corresponding slip efficiency index  $\eta$  was maximum, and a higher average orientation velocity could be obtained per unit vibration intensity.



When the contact surface was a flat surface of 316L stainless steel, the simulation of the slip velocity was carried out by taking the interval of  $-7^\circ \leq \alpha \leq 4^\circ$  in conjunction with the analysis above, as shown in Figure 7.

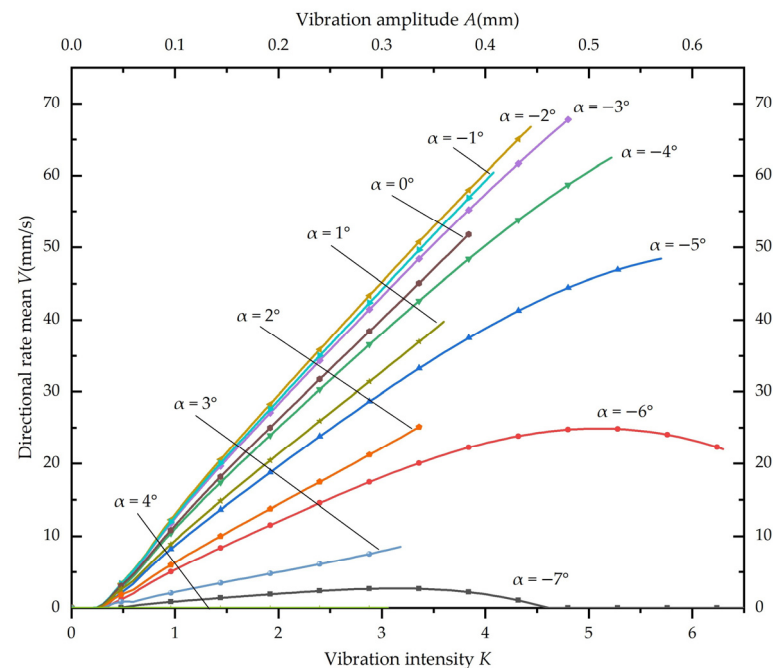


**Figure 7.** The trough is 316L stainless steel.

When the trough plane mounting angle  $\alpha > -3^\circ$ , the maximum vibration intensity  $K_{\max}$  of the fry sliding motion decreased as  $\alpha$  increased. The interval of vibration intensity available for the fry to perform sliding movements was gradually compressed, and the maximum value of the average orientation velocity  $V$  of the fry decreased. When  $\alpha \geq 4^\circ$ , the fry placed backwards and the fry placed forward slid toward the positive direction, and the average directional velocity  $V$  was zero.

When the trough plane mounting angle  $\alpha < -3^\circ$ , the maximum value of the average orientation velocity  $V$  of the fry increased with increasing  $\alpha$ , and the slip efficiency index  $\eta$  increased. When  $\alpha < -7^\circ$ , the fry placed forward and the fry placed backwards slid in opposite directions, and the average directional velocity  $V$  was zero.

When  $\alpha = -2^\circ$ , the corresponding slip efficiency index  $\eta$  was the largest, and a higher average directional velocity  $V$  could be obtained under the unit vibration intensity.

When the contact surface was a PU conveyor belt, the simulation of the slip velocity was calculated by taking the interval of  $-5^\circ \leq \alpha \leq 10^\circ$  in combination with the analysis above, as shown in Figure 8.

When the trough plane installation angle  $\alpha > -8^\circ$ , with the increase in  $\alpha$ , the maximum vibration intensity  $K_{\max}$  of fry sliding motion decreased. The vibration intensity range for the fry to perform a sliding movement was gradually compressed, and the maximum value of the average directional velocity of the fry decreased. When  $\alpha > -5^\circ$ , the backward-placed fry slid together with the forward-placed fry in the forward direction, and their average directional velocity  $V$  was zero.

When the trough plane installation angle  $\alpha < -8^\circ$ , with the increase in  $\alpha$ , the maximum value of the average orientation velocity  $V$  of the fry increased, and the slip efficiency index  $\eta$  increased. When  $\alpha \leq -10^\circ$ , the fry placed forward and the fry placed backward slid in opposite directions, and the average directional velocity  $V$  was zero.

When  $\alpha = -8^\circ$ , the corresponding slip efficiency index  $\eta$  was maximum, and a higher average orientation velocity  $V$  could be obtained per unit vibration intensity.

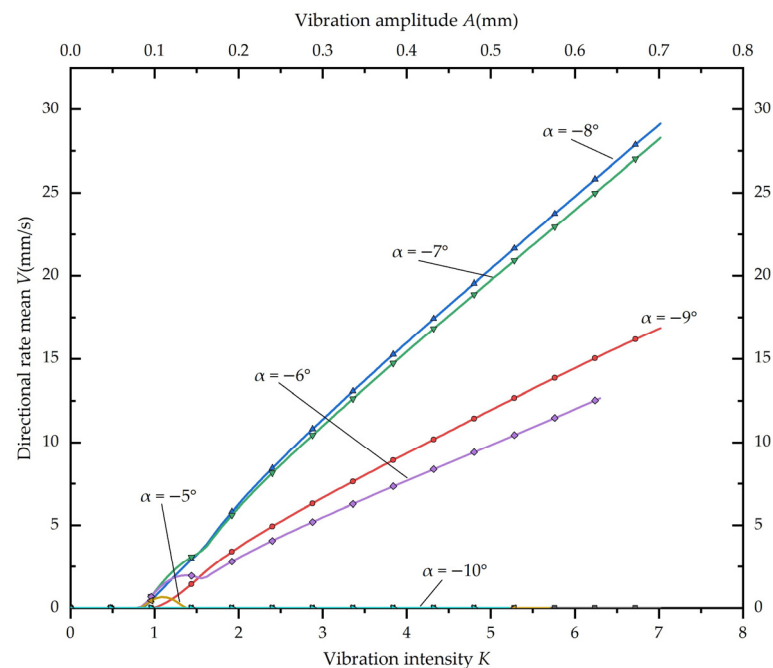


**Figure 8.** The surface of the trough is PU belt.

As could be seen from Figures 6–8, of the three contact surfaces, the fry could obtain the greatest average orientation velocity  $V$  and slip efficiency index on the silicone with many small bumps, the second highest average orientation velocity  $V$  on the 316L stainless steel plate and the worst on the PU tape.

Combined with Figure 5, the greater the difference between the friction angle of the fry on the contact surface, the greater the friction angle between with the scale and against the scale. Furthermore, the greater its average directional velocity, the greater the available angle range. At the same time, the trend of forward slip and backward slip was more obvious. It was easy to identify the head and tail of the fish. In addition, the rougher the contact surface, the greater the vibration intensity required for the fry to start separating.

### 3. Results

In June 2022, the experiment was carried out at the Zijingang Campus of Zhejiang University.

#### 3.1. Test Process

For the fry head and tail orientation device, orientation success and orientation rate were key. Therefore, the orientation success rate  $\varepsilon$  and the orientation rate  $\eta$  were calculated as follows:

$$\varepsilon = \frac{n}{N} \quad (22)$$

$$\eta = \frac{n}{t} \quad (23)$$

Here,  $n$  is the number of successfully oriented fry,  $N$  is the total number of fry and  $t$  is the time taken for orientation.

To find the optimal combination of parameters for the fry head and tail orientation device with a small number of trials, a three-factor, four-level orthogonal experiment was used. In addition, empty columns were added to estimate the test error and to measure the reliability of the test.

A A316L stainless steel surface and a silicone surface with many small bumps were chosen as the trough surface. The angle of inclination of the trough plane relative to the horizontal plane rotating around the Y-axis  $\theta_y = -8^\circ \sim -2^\circ$ ; take the amplitude  $A = 0.4 \sim 0.7$  mm.

Its factor level table is shown in Table 2, and since the trough plane factor term had only two levels, a mixed level orthogonal table  $L_{16}(4^2 \times 2^2)$  was chosen. The test procedure is shown in Figure 9.

**Table 2.** Table of Factor Levels.

Level	Angle $\theta_y$	Amplitude	Materials	Empty
1	$-2^\circ$	0.4 mm	316L	-
2	$-4^\circ$	0.5 mm	Silicone	-
3	$-6^\circ$	0.6 mm	-	-
4	$-8^\circ$	0.7 mm	-	-

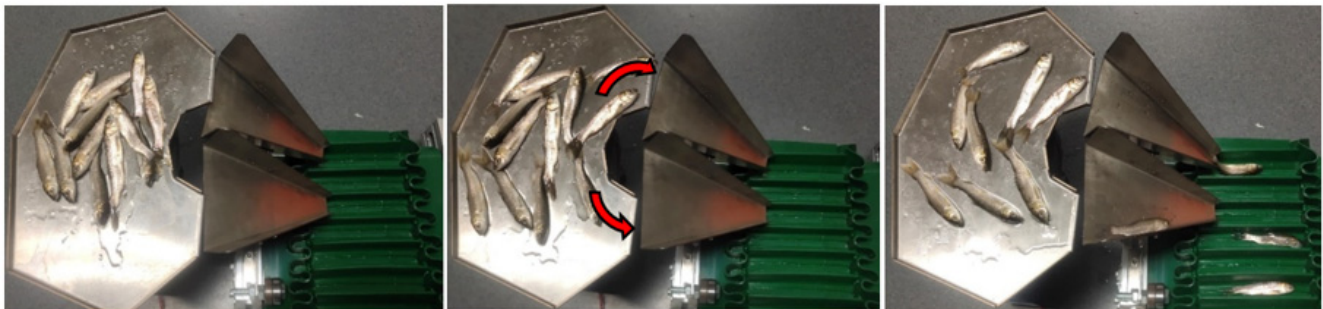


**Figure 9.** The process of head and tail orientation of fry.

### 3.2. Test Results and Analysis

We used MS222 to anesthetize 100 fish ranging from 90–150 mm. At this time, the fry had no response to the external stimulus, and the gill cover was open as normal and stopped swimming [27]. For each test, 30 fish seedlings were randomly selected to record the targeted success rate and the time consumed.

To reduce the effect of other tests, the standard order was randomized to obtain the running order. The tests were carried out in the order of the running sequence. Each group of tests was repeated three times to take the mean value, and the experimental protocol and results are shown in Table 3.

From Table 3, it is clear that there was a positive correlation between orientation rate and orientation success rate. The Minitab(version 18) software was used to analyze the variance on the response average of various factors in Table 3 to the target rate of the directional rate and create the horizontal effect diagram of the factor. As can be seen from Table 4, the  $p$ -values for the significance level of the trough inclination angle  $\theta_y$ , amplitude  $A$  and material were all less than 0.05, which means that the three factors had a significant effect on the fry orientation rate. The  $p$ -value for the significance level of the empty column was greater than the  $p$ -values for the other three factors, indicating that the experimental error was small and the experimental results were reliable.

Figure 10 shows that the orientation rate of fry tended to increase and then decrease as the inclination angle of the trough plane  $\theta_y$  decreased. When the inclination angle was smaller than the critical value, the role of gravity began to dominate. At this time, the displacement of the reverse slip of the fry in the forward and backward directions increased. When the inclination angle was further increased, the forward and backward fry would slip together in the opposite direction, making separation less efficient. The orientation rate of fry tended to gradually increase with increasing amplitude  $A$ . When the inclination angle was near a suitable value, the amplitude increased. Whether it was forward or back to the back, the speed would eventually increase, increasing the fry's orientation rate. However, when the amplitude was too high, the fry would be thrown away from the plane of the trough and would keep hitting it, so the amplitude should not exceed the critical throwing amplitude. When the difference between the friction angle of the scales and the inverse scale increased, the sliding toward the direction of the scales would be faster than the

sliding direction of the inverse scale. Fish with two different orientations were more easily separated, and the machine had a greater orientation rate.

**Table 3.** Experimental protocol and results.

Standard Sequence	Running Sequence	Angle $\theta_y$	Vibration Amplitude $A$	Feeder Plane	Empty	Orientation Speed $\eta$	Success Rate $\varepsilon$
1	16	1 ( $-2^\circ$ )	1 (0.4 mm)	1 (316L)	1	0.30	0.744
2	12	1	2 (0.5 mm)	1	1	0.42	0.756
3	15	1	3 (0.6 mm)	2 (Silicone)	2	0.61	0.800
4	14	1	4 (0.7 mm)	2	2	0.79	0.856
5	7	2 ( $-4^\circ$ )	1	1	2	0.35	0.711
6	8	2	2	1	2	0.42	0.744
7	3	2	3	2	1	0.66	0.900
8	4	2	4	2	1	0.87	0.956
9	9	3 ( $-6^\circ$ )	1	2	1	0.37	0.756
10	1	3	2	2	1	0.48	0.778
11	13	3	3	1	2	0.39	0.722
12	5	3	4	1	2	0.42	0.744
13	2	4 ( $-8^\circ$ )	1	2	2	0.45	0.889
14	11	4	2	2	2	0.53	0.911
15	10	4	3	1	1	0.32	0.700
16	6	4	4	1	1	0.34	0.744

**Table 4.** Formula analysis table of various factors response average.

Variance	Freedom	Sum of Squares	Mean Sum of Squares	F-Value	p-Value
Angle	3	0.083	0.028	8.14	0.011
Amplitude	3	0.115	0.038	11.36	0.004
Material	1	0.202	0.203	59.94	0.000
Empty	1	0.003	0.003	0.74	0.418

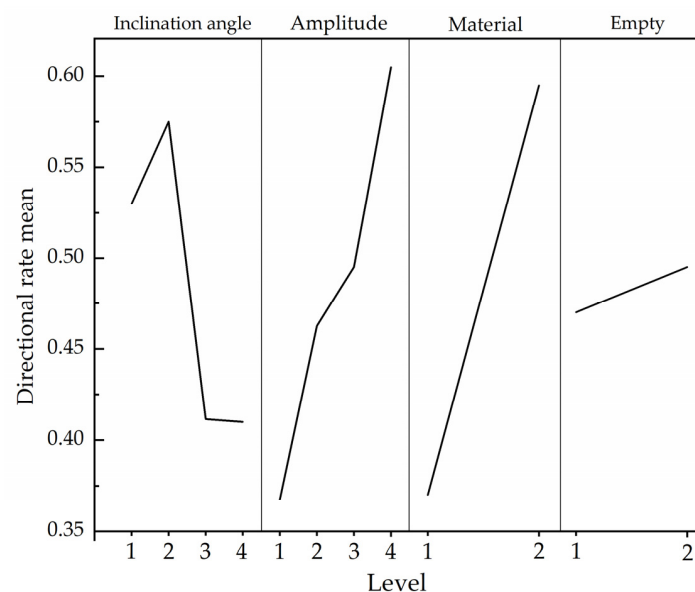


**Figure 10.** Factor level effect map.

The optimal combination of three factors was a graphic tilt angle  $\theta_y$  of  $-4^\circ$ , an amplitude of 0.7 mm, and a graphic plane as the surface with a lot of raised silicone film. Under this parameter combination, the directional device was conducted and verified. Additionally, 30 fry were randomly selected for testing in triplicate, and their average value

was taken. The device had an orientation success rate of 95.6% and an orientation rate of 0.87 tails/s.

#### 4. Discussion

This paper analyzed the movement of fish fry on an electromagnetic vibration. It clarified that the inclination angle, amplitude and material of the trough were the key factors affecting the head and tail orientation effect. By conducting orthogonal tests, the operating parameters of the orientation device were optimized to solve the problem of the head-to-tail orientation of grass carp fry.

Different trough materials produced optimum slip efficiency at different inclination angles. Gravity had a greater effect when the inclination of the trough exceeded a critical value. All fry slid down the slope with a low success rate of orientation. When the inclination of the trough was too small, the frictional effect was greater. It had a high success rate but was inefficient in terms of orientation. In addition, within a certain range, the vibration intensity  $K$  of the electromagnetic feeder increased, and the orientation rate also increased. Its conclusions were consistent with the reference [6]. However, the intensity of vibration  $K$  that produced slip varied for different materials. In the same sliding direction, the fry would slide more easily with the scale direction than against the scale direction. The fish placed forward were more easily distinguishable from those placed backward. The theoretical analysis of slip velocity showed that when the difference in the friction angle between the fry on the contact surface was greater, the average orientation velocity was greater. This was consistent with the findings of references [11,12]. At the same time, the more pronounced the tendency to slide forward and backward, the easier it was to orient the fish's head and tail. In addition, the rougher the contact surface, the greater the intensity of vibration required for the fry to start separating.

The best orientation for this article was a silicone film with many bumps on the surface of the trough. On silicone film, the fry had a large difference in the angle of friction between the subscale and the reverse scale, which was more conducive to head and tail orientation. In addition, the effect of the shape of the surface bumps, the spacing and the thickness of the film on the results could be further explored. Moreover, the study was conducted on grass carp and may not be applicable to other types of fish. The coefficient of friction and the position of the center of gravity were different for each species of fish. Reference [8] showed that reciprocating vibration equipment had a higher success rate in achieving head and tail orientation in adult commercial fish compared to this form of circular vibration. However, further research was needed for young fry. The head and tail orientation device studied in this paper helps to automate the injection process, reducing manual labor, increasing efficiency, improving injection accuracy, reducing fry mortality and laying the foundation for automated fish vaccination.

#### 5. Conclusions

(1) The working mechanism of the fry head and tail orientation was studied, and the frictional characteristics of the scale and inverse scale on different materials were measured. The design of a head and tail orientation device for grass carp fry was based on the difference in torque of the head and tail friction on the center of mass of the fish body.

(2) A force analysis of the fry was carried out to investigate the four states of motion on the trough. The relationship between the vibration intensity of the electromagnetic feeder and the state of fry movement was clarified. The critical vibration strength of the fry in the direction of the scale was less than the critical vibration strength in the direction of the inverse scale.

(3) Based on the theoretical analysis, the simulation calculated that, under different contact surfaces, when the difference between the friction angle of the fry on the contact surface between the scales and inverse scales was larger, the average orientation rate was larger and the angle interval available was also larger. The more obvious the forward and back-to-slip trends, the easier it was to achieve the head and tail orientation.

(4) Head and tail orientation tests were carried out, and the optimum working conditions were: at an inclination angle of  $\beta = 15^\circ$  for the installation of the plate spring, a trough plane inclination angle of  $\theta_y = -4^\circ$ , an amplitude of  $A = 0.7$  mm and a trough plane of silicone film with many bumps on the surface. The orientation speed with the optimal combination of parameters was 0.87 tails/s, and the orientation success rate was 95.6%. This study was only for grass carp; further trials are needed for head-to-tail orientation of other spindle-shaped fry.

**Author Contributions:** Methodology, J.L. and C.L. (Chen Li); software, K.W. and C.L. (Congcong Li); validation, C.L. (Chen Li); formal analysis, K.W. and C.L. (Congcong Li); investigation, C.L. (Chen Li); resources, J.L.; data curation, C.L. (Chen Li); writing—original draft preparation, C.L. (Chen Li); writing—review and editing, W.L. and J.L.; visualization, C.L. (Chen Li); supervision, J.L., Z.Y. and S.Z.; project administration, J.L.; funding acquisition, J.L. and Z.Y. All authors have read and agreed to the published version of the manuscript.

**Funding:** This research was funded by the earmarked fund for China Agriculture Research System (CARS-45-24), and the National Key Research and Development Program of China (Grant No. 2019YFD0900103-05).

**Institutional Review Board Statement:** The maintenance, handling, and experiments conducted on fish during this study were carried out in strict accordance with the guidelines of the Experimental Animal Welfare Ethics Committee of Zhejiang University (no. ZJU20190079).

**Data Availability Statement:** The data presented in this study are available on demand from the second author at (lichen2020@zju.edu.cn).

**Acknowledgments:** The authors gratefully acknowledge the financial support provided by the earmarked fund for the China Agriculture Research System (CARS-45-24) and The National Key Research and Development Program of China (Grant No. 2019YFD0900103-05). We also appreciate the work of the editors and the reviewers of the paper. (e.g., materials used for experiments).

**Conflicts of Interest:** The authors declare no conflict of interest.

## References

1. Nakanishi, T. Preface—Development and use of vaccines for fish. *Fish Shellfish. Immunol.* **2020**, *106*, 218. [CrossRef] [PubMed]
2. Wang, Q.C.; Jin, W.; Xu, Z. Current use and development of fish vaccines in China. *Fish Shellfish. Immunol.* **2020**, *96*, 223–234. [CrossRef] [PubMed]
3. Wang, Q.Y. Fish vaccine technology development and application in China: A review. *J. Dalian Ocean. Univ.* **2022**, *37*, 1–9. [CrossRef]
4. Li, D.D. Study on Automatic Injection Machine for Fish Based on Machine Vision. Master's Thesis, Zhejiang University, Hangzhou, China, 2019.
5. Zhang, J.W.; Chen, Q.Y.; Ou, Y.J.; Zhou, C.S. Research Progress on Pretreatment and Processing Technology of Freshwater Fish in China. *Anhui Agric. Sci.* **2018**, *46*, 25–28. [CrossRef]
6. Xiang, Y.P.; Tan, H.Q.; Wan, P.; Huang, P.F.; Yang, C.X. Theoretical analysis and experimental study about head-tail orientation rule of silver carp on vibration platform. *J. Huazhong Agric. Univ.* **2017**, *36*, 130–138. [CrossRef]
7. Gao, X.X.; Tan, H.Q. Design and experiment of directional transport device of freshwater fish bodies. *Trans. CSAE* **2011**, *27*, 342–347.
8. Liu, W. Equipment Manufacture and Orientation Mechanism Study on Freshwater Fishes' Heads and Backs. Master's Thesis, Huazhong Agricultural University, Wuhan, China, 2013.
9. Webster, J.; Bergman, P. Device and Method for Volitionally Orienting Fish: US5816196A. 1998. Available online: <https://worldwide.espacenet.com/patent/search/family/024516040/publication/US5816196A?q=US5816196A> (accessed on 3 January 2023).
10. Zhang, M. Ordered Arrangement Device for Fish. CN105752659A. 2016. Available online: <https://worldwide.espacenet.com/patent/search/family/056324217/publication/CN105752659A?q=CN105752659A&queryLang=en%3Ade%3Afr> (accessed on 3 January 2023).
11. Wan, P.; Guo, S.Q.; Yang, J.; Zhao, J.W.; Tan, H.Q.; Zhu, M. Horizontal reciprocating vibration method for head-to-tail directional transportation of fresh water fish. *Trans. CSAE* **2021**, *37*, 40–48. [CrossRef]
12. Lin, Q.Y.; Mu, J.C. Initial exploration of fish orientation machinery. *Fish. Mod.* **1980**, *4*, 7–9.
13. Xu, S.B.; Xu, X.Y. A feasibility study on the development of mechanism for the directional transport of fish bodies. *J. Zhejiang Ocean. Univ.* **1990**, *9*, 131–134.



14. Pegoraro, G.; Wadell, L. Fish Feed Apparatus and Method. EP0548383B. 1994. Available online: <https://worldwide.espacenet.com/patent/search/family/008207456/publication/EP0548383A1?q=EP0548383> (accessed on 3 January 2023).
15. Wang, Q.H. Research on the Equipment for Orientation and Cutting Head of Freshwater Fish. Master's Thesis, Wuhan Polytechnic University, Wuhan, China, 2020.
16. Andresen, H.; Eriksson, J.; Hagglund, J.; Hammeren, J.; Kleven, H.; Oppheim, P.; Vaagland, F. Device for Singularization of Fish. EP2820946A. 2015. Available online: <https://worldwide.espacenet.com/patent/search/family/044115125/publication/EP2820946A1?q=EP2820946> (accessed on 3 January 2023).
17. Wenzel, W. Device for Sorting Fish. US4613031. 1986. Available online: <https://worldwide.espacenet.com/patent/search/family/006209443/publication/US4613031A?q=US4613031&queryLang=en%3Ade%3Afr> (accessed on 3 January 2023).
18. Yang, L.; Chen, Z.Y.; Xiao, H.P. Calculation of volume at both ends of liquid bridge between two parallel plates. *Coll. Phys.* **2021**, *12*, 12–14+19. [\[CrossRef\]](#)
19. Geng, A.J.; Li, X.Y.; Hou, J.L.; Zhang, Z.L.; Zhang, J.; Chong, J. Design and experiment of automatic directing garlic planter. *Trans. CSAE* **2018**, *34*, 17–25. [\[CrossRef\]](#)
20. Li, Y.H.; Liu, Q.C.; Li, T.H.; Wu, Y.Q.; Niu, Z.R.; Hou, J.L. Design and experiments of garlic bulbil orientation adjustment device using Jetson Nano processor. *Trans. CSAE* **2021**, *37*, 35–42. [\[CrossRef\]](#)
21. Yu, Y.X.; Zhao, Y.; Zhang, B.; Li, G. Seed metering device based on orienting ordered arrangement in embryo and parameter optimization. *J. Jiangsu Univ. Nat. Sci. Ed.* **2008**, *3*, 194–197.
22. Han, B.; Meng, F.C.; Liang, L.N.; Ge, Y.X.; Xu, H.Y. Performance experiment of directional precision seeding device for japonica rice. *Trans. CSAE* **2015**, *31*, 8–15. [\[CrossRef\]](#)
23. Wang, Y.B.; Zhao, X.G.; Xu, L.M.; Li, C.; Lu, X.; Li, S.J. Experiment and Directional Movement Technology of Corn Seed Based on Electromagnetic Vibration. *Trans. Chin. Soc. Agric. Mach.* **2015**, *45*, 79–88. [\[CrossRef\]](#)
24. Xing, J.J.; Xu, L.M.; Yuan, Q.C.; Ma, S.; Yu, C.C.; Duan, Z.Z. Design and test of pushing device for dent corn seeds directional sowing. *Trans. CSAE* **2018**, *34*, 9–15. [\[CrossRef\]](#)
25. Chen, J.Y. Research on Key Technologies and Mechanisms of Automatic Fish Vaccine Injection Equipment. Master's Thesis, Zhejiang University, Hangzhou, China, 2020.
26. Gu, P.C. Research on feeding speed of electromagnetic vibration feeder. *J. Mech. Electr. Eng.* **2012**, *29*, 790–794.
27. Yu, W.; Wu, J.X.; Lin, H.Z.; Wen, G.L.; Cao, Y.C.; Hu, X.L.; Huang, Z.; Yang, Y.K.; Li, T.; Zhao, W. Anesthetic effect of eugenol on lateolabrax maculatus. *Hebei Fish.* **2020**, *4*, 4–7+11. [\[CrossRef\]](#)

**Disclaimer/Publisher's Note:** The statements, opinions and data contained in all publications are solely those of the individual author(s) and contributor(s) and not of MDPI and/or the editor(s). MDPI and/or the editor(s) disclaim responsibility for any injury to people or property resulting from any ideas, methods, instructions or products referred to in the content.